Available online at www.sciencedirect.com
SCIENCE DIRECT®
Journal of Sound and Vibration 287 (2005) 433–458
JOURNAL OF SOUND AND VIBRATION
www.elsevier.com/locate/jsvi

Responses of discretized systems under narrow band nonstationary random excitations. Part 1: linear problems

Z. Chen, C.W.S. To*

Department of Mechanical Engineering, University of Nebraska, 104N Walter Scott Engineering Center, P.O. Box 880656, Lincoln, NE 68588-0656, USA

Received 26 April 2004; received in revised form 20 October 2004; accepted 11 November 2004
Available online 19 January 2005

Abstract

The extended stochastic central difference (ESCD) method is proposed as a viable alternative for computing linear responses of discretized multi-degrees-of-freedom (mdof) systems under narrow band stationary and nonstationary random disturbances. The method provides a means of controlling the center frequencies and bandwidths of narrow band stationary and nonstationary random excitation processes. It is suitable for larger-scale random response analysis of complicated structures idealized by the finite element method. Its additional important feature is that application of normal mode or complex normal mode analysis or direct numerical integration algorithms such as the fourth-order Runge–Kutta scheme is not required. Examples, including one of flow-induced vibration of a pipe containing a moving fluid are included to demonstrate: (1) the capability of the proposed method and difference between responses of discretized systems under narrow band and wide band random excitations, and (2) its accuracy and efficiency by way of comparison to the Monte Carlo simulation data. Generalization of the ESCD method for computation of responses of nonlinear mdof systems is presented in a companion paper.
© 2004 Elsevier Ltd. All rights reserved.

1. Introduction

Random motion is a very common phenomenon in nature. In engineering design and manufacturing, typical loadings used or that occurred in practice are random in nature. It has

*Corresponding author. Tel.: +1 402 472 1678; fax: +1 402 472 1465.
E-mail address: cto2@unl.edu (C.W.S. To).

0022-460X/$ - see front matter © 2004 Elsevier Ltd. All rights reserved.
doi:10.1016/j.jsv.2004.11.020

been almost five decades since the milestone conference on random vibration held at the Massachusetts Institute of Technology in 1950. During this time, many techniques and methods have been introduced and developed [1,2], among which the stochastic central difference (SCD) method [1] and the stochastic version of the Newmark family of algorithms [3] have been proved to have more advantageous features over the others. The advantages are low computational cost, no restriction on the type of damping in the system, being applicable in conjunction with the finite element analysis (FEA) and, therefore, that it can be applied to complicated structures where analytical solution, employing the normal mode or complex normal mode in the cases involving nonproportional dampings or direct numerical integration algorithm such as the fourth-order Runge–Kutta scheme may prove to be relatively much more expensive.

In the analysis, the types of random vibration problems dealt with to-date have almost exclusively been treated as wide band random processes. While wide band random processes are good approximations to many physical phenomena, there is a wide variety of physical phenomena that have to be categorized as narrow band random processes. For example, flow-induced forces on heat exchanger tubes could be represented by narrow band stationary random processes. A literature survey shows that investigations of systems under narrow band random excitations seem to be relatively limited and have been recommended for further effort [4]. Some of the previous investigations [5,6] are based on pseudo-sinusoidal representation of the narrow band random excitation and have not considered the bandwidth of the excitation as a parameter in their analyses. Tagata [7] suggests that the effects of bandwidth of excitation are very critical and that engineering designs would have to be very conservative and expensive if bandwidth as an important parameter is neglected. Among publications available in the literature, the investigations with narrow band excitations have mainly focused on stationary processes [5–8].

Consequently, the purpose of the investigation reported here was to develop a method that provides the freedom of controlling the center frequencies and bandwidths of narrow band stationary and nonstationary random excitation processes, and to be applicable with the FEA. The objectives of the investigation, however, included the followings. First, a method was to be developed for the determination of linear and nonlinear responses of multi-degrees-of-freedom (mdof) systems under narrow band stationary and nonstationary random excitations. This method was applicable to wide band and narrow band stationary and nonstationary Gaussian random excitation processes. Second, applications of the method are made to engineering systems discretized by the finite element method (FEM). Third, verification and comparison of the obtained results are made to those computed by the Monte Carlo simulation (MCS).

In this paper only responses of linear systems are considered, while responses of nonlinear systems are to be presented in a companion paper [9]. The organization of this paper is as follows. Section 2 introduces the extended stochastic central difference (ESCD) method. For brevity, only representative results are presented in Sections 3–5. Section 3 includes results of a single-degree-of-freedom (sdof) system. Section 4 deals with a beam structure discretized by the FEM. Application of the method is made in Section 5 to the narrow band random response analysis of flow-induced vibration of a pipe containing a moving medium. The latter system is also discretized by the FEM and is an example of a system with nonproportional damping. Concluding remarks are included in Section 6.

2. Extended stochastic central difference method

This section is concerned with the derivation of recursive expressions of the ESCD method for the computation of response statistics of single and mdof systems under wide band and narrow band stationary and nonstationary random excitations. Important issues concerning time step size and stiff systems are addressed.

2.1. Systems under narrow band random excitations

Consider a mdof system under narrow band random excitations, which are obtained from the outputs of filters perturbed by modulated Gaussian white noise excitations. A schematic representation of a sdof system is shown in Fig. 1. The governing matrix equations of motion are

$$M_f\ddot{f} + C_f\dot{f} + K_f f = r(t) = e(t)w(t), \tag{1}$$

$$M_y\ddot{Y} + C_y\dot{Y} + K_y Y = f, \tag{2}$$

where M_f, C_f and K_f are the mass, damping and stiffness matrices of the filters while M_y, C_y and K_y are the mass, damping and stiffness matrices of the mdof system, respectively; $\ddot{f}, \dot{f}$ and f are the random acceleration, velocity and displacement vector of the filters and $\ddot{Y}$, $\dot{Y}$ and Y are the response acceleration, velocity and displacement vectors of the system; and $e(t)$ is a time-dependent deterministic modulating function vector. The zero-mean stationary Gaussian white noise process $w(t)$ has the spectral density S_0. By changing the natural frequencies and damping ratios of the filters and the spectral density of the Gaussian white noise excitation, a variety of narrow band random processes, in the time domain, with different properties such as central frequencies and bandwidths can be obtained.

By employing the same procedures introduced in Refs. [1,3], and after some algebraic manipulation, one has the following recursive expressions accordingly:

$$\begin{aligned} R_y(s+1) = {} & N_{2y}R_y(s)N_{2y}^{\mathrm{T}} + N_{3y}R_y(s-1)N_{3y}^{\mathrm{T}} + (\Delta t)^4 N_{1y}R_f(s)N_{1y}^{\mathrm{T}} \\ & + N_{2y}D_y(s)N_{3y}^{\mathrm{T}} + N_{3y}D_y(s)^{\mathrm{T}}N_{2y}^{\mathrm{T}} + (\Delta t)^2 N_{2y}G(s)N_{1y}^{\mathrm{T}} \\ & + (\Delta t)^2 N_{1y}G(s)^{\mathrm{T}}N_{2y}^{\mathrm{T}} + (\Delta t)^2 N_{3y}H(s)N_{1y}^{\mathrm{T}} \\ & + (\Delta t)^2 N_{1y}H(s)^{\mathrm{T}}N_{3y}^{\mathrm{T}}, \end{aligned} \tag{3}$$

where

$$f_s = f(s), \quad Y_s = Y(s), \quad G(s) = \langle Y_s f_s^{\mathrm{T}} \rangle, \quad H(s) = \langle Y_{s-1} f_s^{\mathrm{T}} \rangle,$$
$$R_f(s) = \langle f_s f_s^{\mathrm{T}} \rangle, \quad R_y(s) = \langle Y_s Y_s^{\mathrm{T}} \rangle,$$

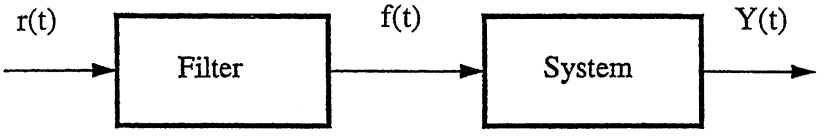

Fig. 1. Schematic model of narrow band random excitation.

$$D_y(s) = \langle Y_s Y_{s-1}^{\mathrm{T}} \rangle = N_{2y} R_y(s-1) + N_{3y} D_y^{\mathrm{T}}(s-1) + (\Delta t)^2 N_{1y} G^{\mathrm{T}}(s-1),$$

$$N_{1y} = [M_y + \tfrac{1}{2}(\Delta t) C_y]^{-1}, \quad N_{2y} = N_{1y}[2M_y - (\Delta t)^2 K_y], \quad N_{3y} = N_{1y}[\tfrac{1}{2}(\Delta t) C_y - M_y].$$

Note that subscripts f and y designate filter and system, respectively. Thus, the last three relations can be applied to the filters by replacing the subscript y with f. For example,

$$N_{1f} = [M_f + \tfrac{1}{2}(\Delta t) C_f]^{-1},$$

and so on. The time step index s is such that $t_{s+1} - t_s = \Delta t$. In the foregoing, the superscript T denotes the transpose of the matrix while the angular brackets designate the ensemble average or mathematical expectation.

It may be appropriate to note that the major differences between the ESCD method for narrow band excitations and the SCD method for wide band disturbances are the presences of the $G(s)$ and $H(s)$ terms, which are the vehicles carrying frequencies and band width content from the filters to system. Before applying Eq. (3), recursive relations of $G(s)$ and $H(s)$ have to be derived. To this end one substitutes

$$Y(s) = (\Delta t)^2 N_{1y} f(s-1) + N_{2y} Y(s-1) + N_{3y} Y(s-2)$$

into the expression for $G(s)$ so that

$$\begin{aligned} G(s) &= \langle Y(s) f(s)^{\mathrm{T}} \rangle \\ &= \langle [(\Delta t)^2 N_{1y} f(s-1) + N_{2y} Y(s-1) + N_{3y} Y(s-2)] f(s)^{\mathrm{T}} \rangle \\ &= (\Delta t)^2 N_{1y} D_f(s)^{\mathrm{T}} + N_{2y} H(s) + N_{3y} \langle Y(s-2) f(s)^{\mathrm{T}} \rangle. \end{aligned} \tag{4}$$

Similarly, one can substitute the recursive expression for $f(s)^{\mathrm{T}}$ or simply f_s^{T}, which can be shown to be [1]

$$f(s)^{\mathrm{T}} = (\Delta t)^2 r(s-1)^{\mathrm{T}} N_{1f}^{\mathrm{T}} + f(s-1)^{\mathrm{T}} N_{2f}^{\mathrm{T}} + f(s-2)^{\mathrm{T}} N_{3f}^{\mathrm{T}},$$

into the last term of Eq. (4) such that

$$\begin{aligned} \langle Y(s-2) f(s)^{\mathrm{T}} \rangle &= \langle Y(s-2)[(\Delta t)^2 r(s-1)^{\mathrm{T}} N_{1f}^{\mathrm{T}} + f(s-1)^{\mathrm{T}} N_{2f}^{\mathrm{T}} + f(s-2)^{\mathrm{T}} N_{3f}^{\mathrm{T}}] \rangle \\ &= H(s-1) N_{2f}^{\mathrm{T}} + G(s-2) N_{3f}^{\mathrm{T}}, \end{aligned} \tag{5}$$

in which the fact that the term associated with $\langle r(s)^{\mathrm{T}} \rangle$ is zero has been used. After combining Eqs. (4) and (5), it leads to

$$G(s) = (\Delta t)^2 N_{1y} D_f(s)^{\mathrm{T}} + N_{2y} H(s) + N_{3y} H(s-1) N_{2f}^{\mathrm{T}} + N_{3y} G(s-2) N_{3f}^{\mathrm{T}}. \tag{6}$$

A similar operation can be performed on the term $H(s)$ in Eq. (3). Thus, one can show that

$$\begin{aligned} H(s) &= \langle Y(s-1) f(s)^{\mathrm{T}} \rangle \\ &= \langle Y(s-1)[(\Delta t)^2 r(s-1)^{\mathrm{T}} N_{1f}^{\mathrm{T}} + f(s-1)^{\mathrm{T}} N_{2f}^{\mathrm{T}} + f(s-2)^{\mathrm{T}} N_{3f}^{\mathrm{T}}] \rangle \\ &= G(s-1) N_{2f}^{\mathrm{T}} + \langle Y(s-1) f(s-2)^{\mathrm{T}} \rangle N_{3f}^{\mathrm{T}}. \end{aligned} \tag{7}$$

Upon application of Eq. (5) to the last term on the right-hand side (RHS) of Eq. (7) one has

$$\begin{aligned}\langle Y(s-1)f(s-2)^{\mathrm{T}}\rangle &= \langle[(\Delta t)^2 N_{1y} f(s-2) + N_{2y} Y(s-2) + N_{3y} Y(s-3)]f(s-2)^{\mathrm{T}}\rangle \\ &= (\Delta t)^2 N_{1y} R_f(s-2) + N_{2y} G(s-2) + N_{3y} H(s-2). \end{aligned} \tag{8}$$

Then substituting Eq. (8) into Eq. (7) gives

$$\begin{aligned} H(s) = {} & G(s-1)N_{2f}^{\mathrm{T}} + (\Delta t)^2 N_{1y} R_f(s-2) N_{3f}^{\mathrm{T}} + N_{2y} G(s-2) N_{3f}^{\mathrm{T}} \\ & + N_{3y} H(s-2) N_{3f}^{\mathrm{T}}. \end{aligned} \tag{9}$$

In the above operations, the ensemble average of the narrow band random force vector has been assumed to be zero. If the input to the system does not have a zero ensemble average, it can be considered with due modification to the central difference equation and the remaining steps can be found in Ref. [10].

2.2. Time step size and stiff systems under narrow band random excitations

The relation between the time step size Δt and the natural frequency ω of the system under wide random excitations has been investigated by To and Liu [11]. It has been found that as the natural frequency reduces to a small value the time step size Δt approaches unity. The relation may be written as

$$\Delta t = 0.83 - 0.72 \log_{10}\omega, \quad 1.0 \leqslant \omega < 5.0, \tag{10a}$$

$$\Delta t = 1.0 - 0.053\omega - 0.12\omega^2, \quad \omega \leqslant 1.0. \tag{10b}$$

Eq. (10) does not include a formula for $\omega \geqslant 5.0$ because if the angular natural frequency is higher than 5.0, the time step size becomes too small to be computationally effective. When the angular natural frequency is higher than 5.0, the time coordinate transformation introduced in Ref. [12] should be used. Note that in Eq. (10) the time step size Δt is in seconds and the angular frequency ω is in radian per second.

For stiff systems under wide band random excitations, a computational strategy known as the time coordinate transformation (TCT) was employed in Ref. [12].

It is natural therefore to ask if Eq. (10) and the TCT remain valid and applicable in stiff systems excited by narrow band stationary and nonstationary random disturbances. A detailed parametric study was conducted during the investigation. It was observed that, indeed, the relation for the time step size defined by Eq. (10) and TCT for stiff systems are applicable to cases involving narrow band stationary and nonstationary random excitations.

In closing, it suffices to say that the significance of the TCT is such that very stiff systems can now be dealt with by using the ESCD method. Without the TCT the time step sizes for stiff systems can often lead to computational instability or render determination of recursive responses impossible.

2.3. Recursive narrow band random force vector

Although the center frequency and bandwidth of the filter response can be adjusted by changing the natural frequency and damping ratio of the filter, the amplitude and the shape of amplitude

for nonstationary response cannot be conveniently and simply controlled without further modification. Thus, it is imperative to develop a technique of providing narrow band random forces which can be conveniently controlled.

To begin with, one makes use of Eq. (3) of Ref. [12] for the filter. It is understood that if the system parameters of the filter, M_f, C_f and K_f are constant the recursive covariance matrix of responses, $R(s+1)$, can only change with the variation of the excitation matrix $B(s) = 2\pi S_0 e(s)e(s)^{\mathrm{T}}$. In turn, it can only change with the envelope function vector $e(s)$ and spectral density S_0 of the Gaussian white noise excitation. The goal now is to find an envelope function vector $e(s)$, which can produce a desired covariance matrix $R_f(s)$. In fact, there is a unique $B(s)$ corresponding to a desired response of the filter $R_f(s)$ because Eq. (3) of Ref. [12] is linear. Examining the latter equation carefully, one could find that the envelope function vector $e(s)$ does not have to be determined because it is the resulting narrow band random vector process from the filter, that is required for the system rather than the Gaussian white noise input to the filter. In other words, the envelope function vector of interest is associated with the narrow band random vector process from the filter. Thus, the envelope function vector of the covariance of the narrow band random vector process from the filter is desired. To do this, let

$$R_f(s) = [e_f(s)e_f^{\mathrm{T}}(s)]I, \tag{11}$$

where $R_f(s)$ and $e_f(s)$ are the response covariance and envelope function vector of the narrow band random processes of the filter while I is a constant.

By inspection of Eq. (11) itself, it seems that the effect of frequency and bandwidth, therefore damping ratio, has been lost in the process because it does not include N_{1f}, N_{2f} and N_{3f} which contain features of the filter. However, upon close examination one finds that the characteristics of the filter are indeed retained in $G(s)$ and $H(s)$ which carry the frequency and bandwidth characters into the system responses. Thus, the recursive relation representing the narrow band random vector process are

$$R_f(s+1) = [e_f(s+1)e_f^{\mathrm{T}}(s+1)]I, \tag{12}$$

$$D_f(s) = N_{3f}D_f(s-1) + N_{2f}R_f(s-1) \tag{13}$$

which are the covariance expressions of the input forces to the system.

By applying different envelope functions $e_f(s)$, constant I, the natural frequencies of the filters and the ratios of damping to mass, a variety of different shapes, spectral densities, center frequencies and band widths of the narrow band random processes from the filters can be obtained. This is a unique and efficient feature of the presently proposed ESCD method. Note that to provide a similar feature in MCS is much more difficult, if not impossible. With this feature, the ESCD method can be applied to the analysis of systems under narrow band random excitations.

3. Single degree of freedom systems

For applications of the ESCD method, the simplest case is a sdof system. In this section, responses of such a system under narrow band stationary and nonstationary random excitations

are obtained using the ESCD method. Data obtained by the MCS for some representative cases are included for direct comparison.

Analytical solution of the response of a linear sdof system excited by a narrow band stationary random excitation has been presented in Ref. [13], for example. However, an exact analytical solution of the same system under narrow band nonstationary random excitation seems to be unavailable at the present time. Therefore, the current phase of the investigation reported in this section has three main objectives. Firstly, the results for the system under narrow band stationary random excitation obtained by the ESCD method are verified by the analytical solution [13] and MCS data. The relationships between the time step sizes and the natural frequencies of the filter and system are established. The effect of damping ratio of the filter on the time step is evaluated. Secondly, the issue of interpolation of the input to the system, that is the output from the filter is examined. Thirdly, comparisons are made of responses of systems under narrow band and wide band nonstationary random excitations. The above three main objectives are pursued in the following subsections.

3.1. Relationship between time step size and natural frequency

Tables 1 and 2 contain results of some representative systems under narrow band stationary random excitations. Note that the subscripts f and s in the tables refer to the filter and system, respectively. Results for the study of the effect of parameters of filters on the time step size of the system are presented in Table 1. The parameters which were kept constant are as follows: $M_y = 1.0$, $K_y = 1.0$, $C_y = 0.0246875$, $M_f = 1.0$, $C_f = 0.029625$ and the spectral density of the Gaussian white noise applied to the filter, $S_0 = 1.0$, such that the variance of the discrete white noise process is $\langle w^2(0)\rangle = 2\pi$. From this table, it is clear that the natural frequency of the filter does not affect the time step size of the system and that the time step size of the system agrees with Eq. (10). It is also shown in this table that the results computed by the ESCD method and denoted by SCD

Table 1
Effect of filter parameters on time step size

ω_f	ω_s	Δt_f	Δt_s	Variance of response (exact)	Variance of response (SCD)
0.50	1.0	0.945	0.83	61.1	60.8
0.71	1.0	0.910	0.83	336.6	336.2
0.87	1.0	0.860	0.83	2322.7	2322.7
1.00	1.0	0.830	0.83	79,146.0	79,262.0
1.12	1.0	0.800	0.83	5040.7	5027.0
1.23	1.0	0.770	0.83	1757.0	1739.0
1.42	1.0	0.733	0.83	718.0	718.1
2.00	1.0	0.613	0.83	273.2	273.0
3.00	1.0	0.480	0.83	175.9	176.0
4.00	1.0	0.390	0.83	152.3	153.4
5.00	1.0	0.328	0.83	142.7	142.7
10.0	1.0	0.181	0.83	130.9	131.5
20.0	1.0	0.095	0.83	128.2	127.1

Table 2
Effect of natural frequency of system on time step size

M_s	ω_s	Δt_s	Variance of response (exact)	Variance of response (SCD)	Variance of response (MCS)
1.0	0.500	0.935	733.8	733.2	723
	0.707	0.905	546.0	542.0	550
	0.820	0.875	339.0	339.0	345
	1.00	0.831	718.4	716.7	700
	1.414	0.721	79,117.0	79,967.0	78,500
	2.00	0.610	84.8	83.5	83
	3.00	0.486	5.5	5.5	5.7
	4.00	0.398	1.2	1.3	1.2
0.1	10.0	0.182	2.2	2.3	1.9
	20.0	0.094	0.13	0.15	0.12

$\omega_f = 1.414$, $M_f = 1.0$, $C_f = 0.029625$, $K_s = 2.0$, $C_s = 0.0246875$

(henceforth, SCD in the tables and figures refers to results obtained by the ESCD method) in the tables agree very well with the exact solutions [13]. Table 2 includes results of a parametric study of the effect of natural frequencies of systems on its time step size. It also provides responses of various systems under narrow band random excitations with center frequency of 1.414 rad/s. From the table, one can observe that the time step size of the system indeed follows the relation defined by Eq. (10). It is noted that the results computed by the ESCD method and exact solutions have an excellent agreement. Results obtained by using the MCS are also included in Table 2. In the MCS, every solution was obtained with 200 realizations each of which has 25,600 points. The MCS results agree well with the exact solutions.

3.2. Interpolation of system input

In general, because the time step size is associated with natural frequency, the natural frequencies of filter and system are generally different such that the time step size of the system is different from that of the filter. In other words, an output from the filter cannot be directly used as an input to the system since the time steps of the filter and the system are not equal. To resolve this problem, one can adopt the interpolation or extrapolation to adjust the time step of the filter so that it can be applied to the computation of the response of the system. In this investigation an interpolation strategy is applied. It will be shown in the following subsections that such a strategy is very efficient and accurate.

3.3. System under nonstationary random excitation

In this subsection, results for two cases were obtained. The first case is concerned with the effect of various natural frequencies on the responses of the system. This system is subjected to a narrow band random force with center frequency of 1 rad/s. The results are presented in Figs. 2–4. The second case deals a system in resonance at a frequency of 0.5 rad/s. The results are presented in

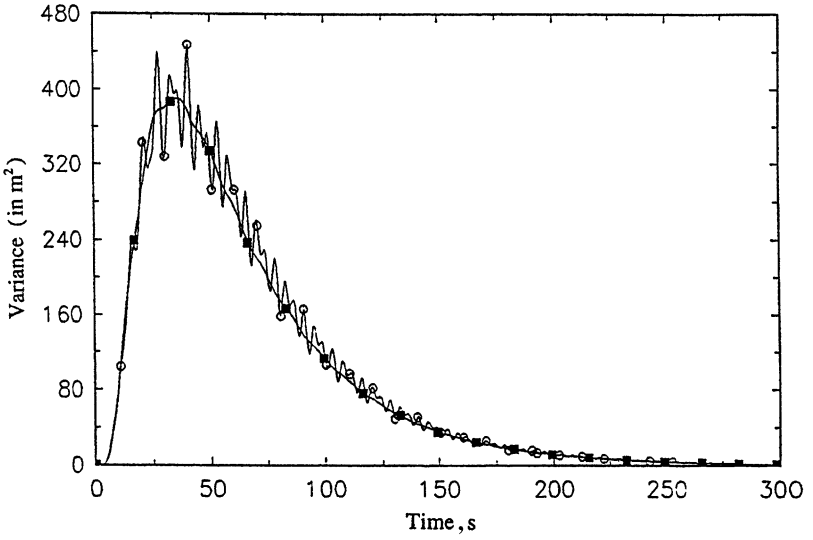

Fig. 2. Displacement response of system with $\omega_f = 1.0\,\mathrm{rad/s}$, $\zeta_f = 0.00985$, $\omega_s = 0.5\,\mathrm{rad/s}$, $\zeta_s = 0.0124$; Simulation (○), and SCD (■).

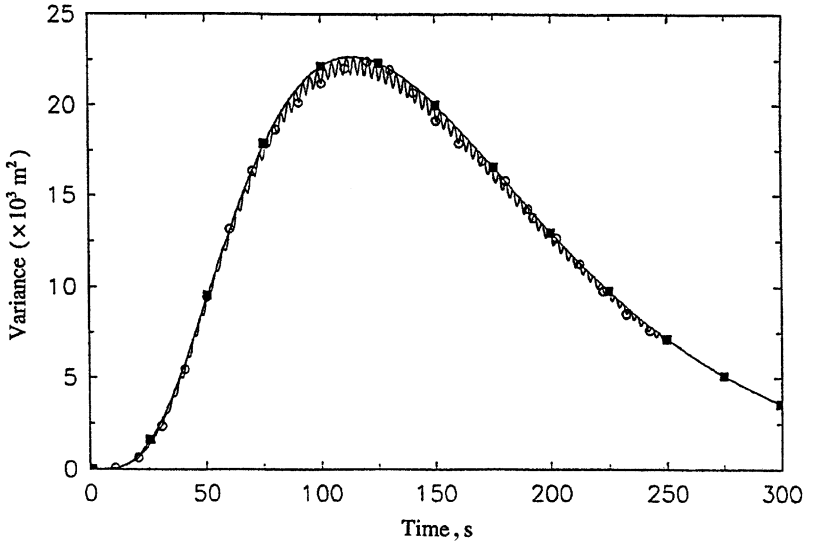

Fig. 3. Resonant displacement response of system with $\omega_f = 1.0\,\mathrm{rad/s}$, $\zeta_f = 0.00985$, $\omega_s = 1.0\,\mathrm{rad/s}$, $\zeta_s = 0.0124$. Simulation (○), and SCD (■).

Fig. 5. It may be appropriate to note that the MCS results in these figures and subsequent ones show significant local fluctuations while those by the ESCD method indicate smooth behavior of the response variance with time. The local fluctuations of the MCS results have to do with the fact that a pseudo-random number generator has been employed and that 200 realizations of the

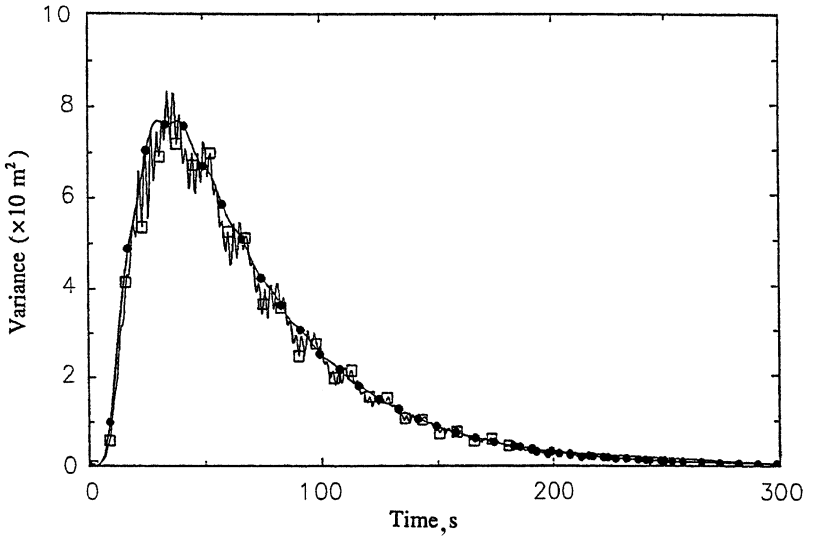

Fig. 4. Displacement response of system with $\omega_f = 1.0\,\mathrm{rad/s}$, $\zeta_f = 0.00985$, $\omega_s = 1.4\,\mathrm{rad/s}$, $\zeta_s = 0.0124$: MCS (□), and SCD (◆).

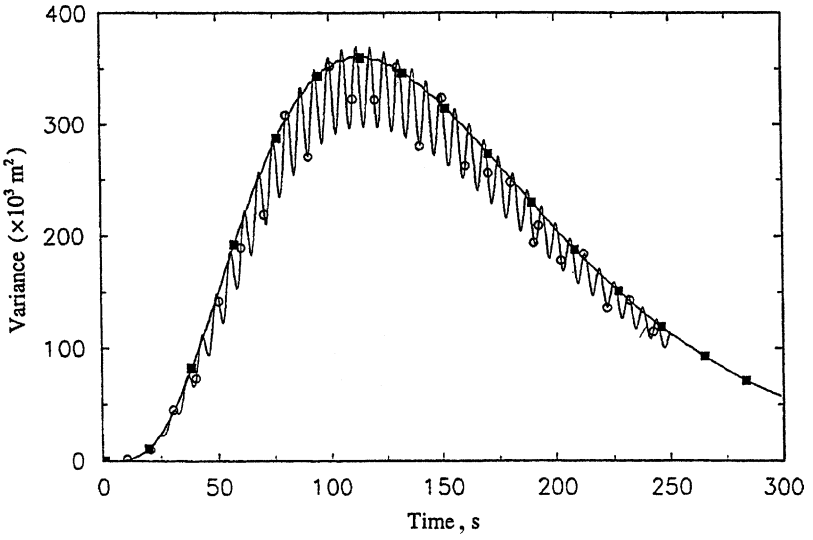

Fig. 5. Resonant displacement response of system with $\omega_f = 0.5\,\mathrm{rad/s}$, $\zeta_f = 0.00985$, $\omega_s = 0.5\,\mathrm{rad/s}$, $\zeta_s = 0.0124$: Simulation (○), and SCD (■).

random responses were considered in the MCS. In other words, the local fluctuations are intrinsic in the MCS and therefore cannot be avoided.

In the above results, the input to the system is a narrow band random excitation which is the output of a filter excited by a modulated Gaussian white noise process. The input to the filter is

$$r = e(t)w(t), \quad \langle w^2(0)\rangle = 2\pi S_0, \quad e(t) = 4.0(\mathrm{e}^{-0.05t} - \mathrm{e}^{-0.1t}), \tag{14}$$

in which $S_0 = 1.0$ has been applied. In the MCS, again, every solution was obtained with 200 realizations, each of which has 25,600 points. It should be pointed out that in the MCS, the computation time was about 40 min while that using the ESCD method was less than a second. The computing machine used was a Silicon Graphics engineering workstation with 64 MB RAM and 60 MHz single central processor. Figs. 3 and 5 include results of the two resonant cases with frequencies of 1.0 and 0.5 rad/s, respectively. In these two cases the same bandwidth ζ_f of narrow band inputs and same damping ratios of the system were employed. Note that the amplitudes of the responses are very different. Comparing Fig. 3 with the two corresponding nonresonant cases, that is, Figs. 2 and 4, it is evident that their responses are very much different as one expects. It is observed that the results obtained by the ESCD method and MCS are very much in agreement.

3.4. Effect of bandwidth of narrow band nonstationary random excitation

Computations for two examples were conducted for the comparison between responses of the system to narrow band and wide band random excitations. The first example has a natural frequency of 1.0 rad/s. In the second example the system has been chosen to have different natural frequencies of 2.0, 3.0 and 4.0 rad/s. Wide band input to the system is a modulated stationary Gaussian white noise excitation defined by Eq. (14), whereas the narrow band input to the system is given by

$$f = e(t)\sqrt{I}, \quad I = 2\pi, \quad e(t) = 4.0(\mathrm{e}^{-0.05t} - \mathrm{e}^{-0.1t}), \tag{15}$$

where I can be used to adjust the amplitude. By inspection of Eqs. (14) and (15), one notices that the modulating functions are identical. The purpose of these choices is to eliminate the effect of amplitude difference between the modulated white noise and modulated narrow band inputs to the filter and system. The time step sizes used are determined by Eq. (10). Two different center frequencies are selected for each example. They are $\omega_f = 1.0$ rad/s for the first example and $\omega_f = 3.0$ rad/s for the second example. Computed results of the first example are presented in Figs. 6 and 7, while those of the second are shown in Fig. 8. Note that owing to the large difference in amplitudes, Figs. 6 and 7 are not presented in a single figure. Comparing Figs. 6 and 7 one observes that not only the amplitudes are very much different but also the times at which the peaks occur are changed. The peaks of resonant cases occur at much later times than that in the nonresonant case. It is also observed that the differences between resonant responses of the system under narrow band excitations and those under white noise excitation in the first example are significantly larger than those in the second example. This indicates that the aforementioned difference decreases with increasing natural frequency.

From the foregoing, one observes that the differences between the responses of the system under narrow band and wide band random excitations are very significant. The conclusion to be drawn at this stage is that correct representation of the excitation process is very important.

4. Responses of discretized beam structure

The discretized cantilever beam studied in Ref. [12] is investigated. It should be pointed out that the results in Ref. [12] are concerned with wide band random excitations applied at the clamped

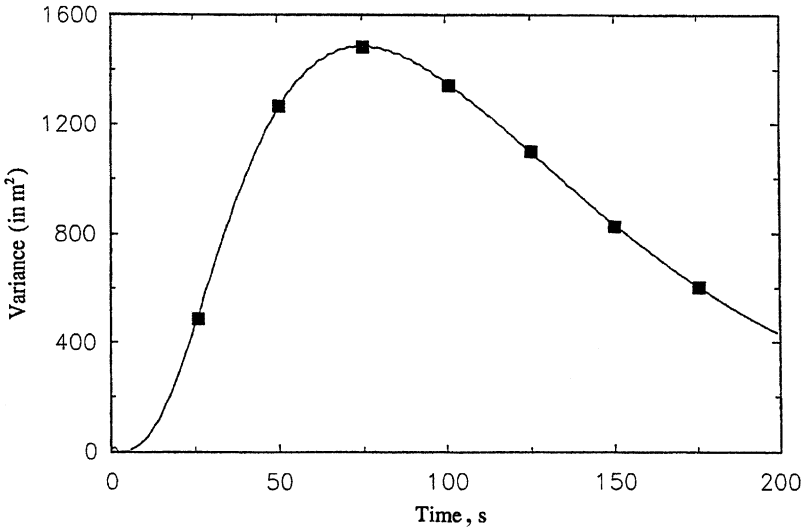

Fig. 6. Effect of bandwidth on variance response for narrow band case with $\omega_f = 1.0\,\text{rad/s}$, $\zeta_f = 0.01$, $\omega_s = 1.0\,\text{rad/s}$, $\zeta_s = 0.01$; SCD (■).

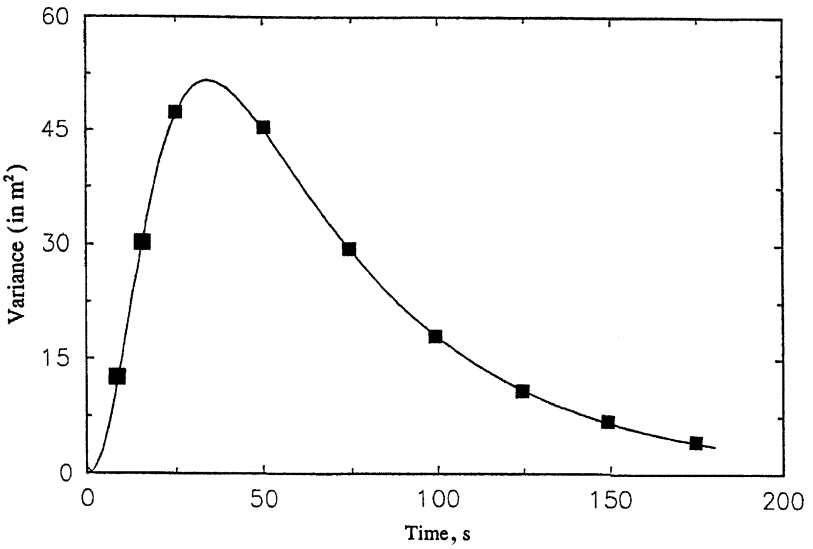

Fig. 7. Effect of bandwidth on variance response for modulated white noise case with $\omega_s = 1.0\,\text{rad/s}$, $\zeta_s = 0.01$; SCD (■).

end. The focus in the present investigation is, however, on responses of the discretized beam structure under narrow band random excitations applied at the free end. The ESCD method and TCT in Section 2 are applied here. The obtained results by the ESCD method are compared with those computed by the MCS.

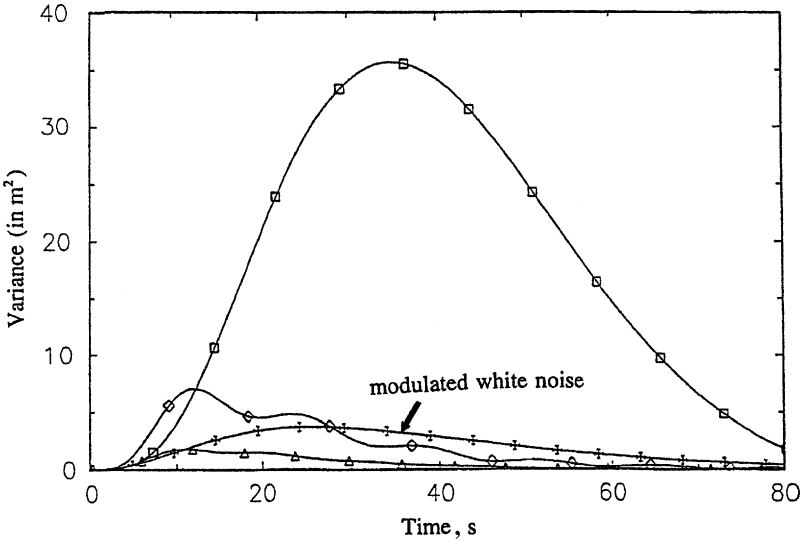

Fig. 8. Variance response of system under nonstationary narrow band and modulated white noise excitations with $\omega_f = 3.0\,\text{rad/s}$, $\zeta_f = 0.01$, $\zeta_s = 0.01$. $\omega_s = 4.0\,\text{rad/s}$ (△), $\omega_s = 3.0\,\text{rad/s}$ (□), $\omega_s = 2.0\,\text{rad/s}$ (◇), and $\omega_s = 3.0\,\text{rad/s}$ (+).

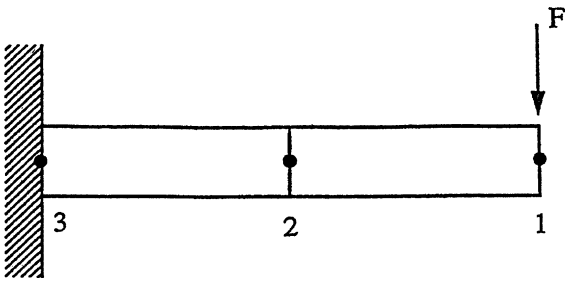

Fig. 9. Discretized cantilever beam structure.

4.1. Discretized beam structure

For illustration purpose the cantilever beam shown in Fig. 9 is approximated by two 2-node beam elements. Every node has three dof, namely, axial displacement u, flexural displacement v and rotation about z-axis θ. For completeness, the element matrices are given below. The consistent element mass matrix is

$$[m] = \frac{\rho A \ell}{420}\begin{bmatrix} 140 & 0 & 0 & 70 & 0 & 0 \\ 0 & 156 & 22\ell & 0 & 54 & -13\ell \\ 0 & 22\ell & 4\ell^2 & 0 & 13\ell & -3\ell^2 \\ 70 & 0 & 0 & 140 & 0 & 0 \\ 0 & 54 & 13\ell & 0 & 156 & -22\ell \\ 0 & -13\ell & -3\ell^2 & 0 & -22\ell & 4\ell^2 \end{bmatrix}, \tag{16}$$

where ρ is the mass density, A the cross-sectional area, and ℓ the length of the element. The consistent element stiffness matrix is given by

$$[k] = \begin{bmatrix} a & 0 & 0 & -a & 0 & 0 \\ 0 & 12b & 6\ell b & 0 & -12b & 6\ell b \\ 0 & 6\ell b & 4\ell^2 b & 0 & -6\ell b & 2\ell^2 b \\ -a & 0 & 0 & a & 0 & 0 \\ 0 & -12b & -6\ell b & 0 & 12b & -6\ell b \\ 0 & 6\ell b & 2\ell^2 b & 0 & -6\ell b & 4\ell^2 b \end{bmatrix}, \tag{17}$$

in which a and b are defined as

$$a = \frac{EA}{\ell}, \quad b = \frac{EI_b}{\ell^3}$$

with E being the Young's modulus and I_b the second moment of area of the cross-section of the beam.

The nodal displacement vector accompanying Eqs. (16) and (17) is

$$\{q\} = [u_i, v_i, \theta_i, u_{i+1}, v_{i+1}, \theta_{i+1}]^{\mathrm{T}},$$

where i is an integer.

Based on the element consistent mass and stiffness matrices, $[m]$ and $[k]$ the assembled mass and stiffness matrices can be obtained

$$[M] = \sum_{e=1}^{N+1} [M]_e, \quad [K] = \sum_{e=1}^{N+1} [K]_e, \tag{18}$$

where the subscript e denotes the element number, $[M]_e$ and $[K]_e$ have the same order as the assembled mass matrix $[M]$ and stiffness matrix $[K]$, respectively. The nonzero elements in the latter matrices are only those in rows and columns that correspond to element degrees of freedom.

For simplicity, the damping matrix is assumed to be proportional, defined as

$$[C] = [M] \sum_{p} \lambda_p [M^{-1}K]^p, \tag{19}$$

where λ_p are constants to be determined and $p = 0, 1, 2, \ldots$. The upper limit of the summation is not defined as it varies from one system to another.

The governing matrix equation of motion in terms of the global–nodal displacement, velocity and acceleration vectors is

$$[M]\{\ddot{Y}\} + [C]\{\dot{Y}\} + [K]\{Y\} = \{F\}, \tag{20}$$

where $\{F\}$ is the vector of consistent nodal forces due to the external random excitations and $\{Y\}$ the global nodal displacement vector. Clearly, Eq. (20) is similar in form to Eq. (2).

The excitation vector on the RHS of equation (20) may be defined as

$$\{F\} = [0 \quad -e(t)\sqrt{I_f} \cdots 0]^{\mathrm{T}}, \tag{21a}$$

where now $e(t)$ is a scalar deterministic modulating function which is given as

$$e(t) = E_r(e^{-\alpha_1 t} - e^{-\alpha_2 t}) \tag{21b}$$

in which α_1 and α_2 are positive constants satisfying $\alpha_1 < \alpha_2$, and E_r is a constant used to normalize $e(t)$ such that $max\{e(t)\} = 1.0$.

With the definition of $[C]$ in Eq. (19) the following algebraic equations can be written to determine constants λ_p:

$$2\zeta_i\omega_i = \sum_p \lambda_p \omega_i^{2p}, \tag{22}$$

or in matrix notation

$$[\lambda_0 \ \ \lambda_1 \ \ \lambda_2 \ \ \cdots]^{\mathrm{T}} = 2\Xi^{-1}[\zeta_1 \ \ \zeta_2 \ \ \zeta_3 \ \ \cdots]^{\mathrm{T}},$$

where Ξ is a square matrix with components $\Xi_{ij} = \omega_i^{2j-3}$, ω_i and ζ_i are the ith natural frequency and modal damping ratio, respectively. As many equations (22) must be included as there are specified modal damping ratios. More detailed discussion on the damping matrix can be found in Ref. [12,14]. It only suffices to state that the ESCD method does not require the modal or complex modal analysis. The modal damping ratios are selected here because they are readily available in Ref. [12]. In the present investigation, damping matrix of the discretized beam structure with $p = 0, 1$ is adopted. The results obtained by the ESCD method and denoted as SCD are compared with those evaluated by the MCS.

The beam structure has the following properties: density of the material $\rho = 7860.0\,\mathrm{kg/m^3}$, Young's modulus of elasticity $E = 2.07 \times 10^{11}\,\mathrm{N/m^2}$, cross-sectional area $A = 6.25 \times 10^{-4}\,\mathrm{m^2}$, moment of inertia of cross-section $I_b = 3.26 \times 10^{-8}\,\mathrm{m^4}$, and length $L = 1\,\mathrm{m}$.

The modulating function $e(t)$ is chosen as

$$e(t) = 9.4815(e^{-45t} - e^{-60t}) \tag{23}$$

and the duration of excitation as $t_p = 0.30\,\mathrm{s}$. Note that the fundamental period, $T_1 = 2\pi/\omega_1$, is 0.04819 s and therefore the duration of excitation chosen above is slightly more than 6 times the fundamental period. The first five modal damping ratios of the beam structure are included in the computation: $\zeta_1 = \zeta_2 = 0.05$, $\zeta_3 = 0.1413$, $\zeta_4 = 0.4049$, and $\zeta_5 = 0.4142$. The two independent coefficients of the damping matrix are: $\lambda_m = 11.3379$ and $\lambda_k = 0.0001$. For this problem there are 6 dof. The six natural frequencies of the discretized beam structure are: $\omega_1 = 130.3777\,\mathrm{rad/s}$, $\omega_2 = 823.5985\,\mathrm{rad/s}$, $\omega_3 = 2785.5606\,\mathrm{rad/s}$, $\omega_4 = 8084.8891\,\mathrm{rad/s}$, $\omega_5 = 8269.5425\,\mathrm{rad/s}$, and $\omega_6 = \Omega = 28888.7357\,\mathrm{rad/s}$.

It may be appropriate to note that since the formulation is based on linear theory, the following condition should be satisfied:

$$\max\{\langle Y_L^2(t)\rangle\} \leqslant \left(\frac{5L}{100}\right)^2,$$

where $\langle Y_L^2(t)\rangle$ is the variance of displacement at the free end of the beam structure.

4.2. Narrow band nonstationary random responses

A program of numerical tests was designed to examine the efficiency and accuracy of the ESCD method. For illustration purpose, only a sdof filter is employed in the computation. The center frequency of the filter is selected in such a way that the fundamental frequency of the discretized beam is excited. The center frequency ω_f and damping ratio ζ_f of the filter are 130.38 rad/s and 0.05 respectively. The sdof filter is excited by a modulated Gaussian white noise process. The latter is given by

$$r(t) = e(t)w(t), \quad \langle w^2(0)\rangle = 2\pi \times 10^{10}, \quad e(t) = 9.4815(\mathrm{e}^{-45t} - \mathrm{e}^{-60t}). \tag{24}$$

The results by the ESCD method, in which $\Delta\tau = 1.0$ is the dimensionless time step after the application of the TCT, are presented in Figs. 10 and 11. Results obtained by the MCS are also included in the figures for comparison. Note that, for brevity, only a representative number of variances of responses are presented. It may be appropriate to point out that for every case the computation time required by the ESCD method is about 3.5 min while that by the MCS is approximately 5.2 h. The computing machine used for the investigation is the Silicon Graphics workstation briefly mentioned in the last section.

With reference to the figures presented in this subsection and the computation times quoted in the foregoing, one may conclude that the ESCD method is very accurate and efficient compared with the MCS.

4.3. Effect of bandwidth of excitation processes

The aim of the study in this subsection is to examine the effect of bandwidth of the excitation process from the single dof filter on the responses of the discretized beam structure. The filter

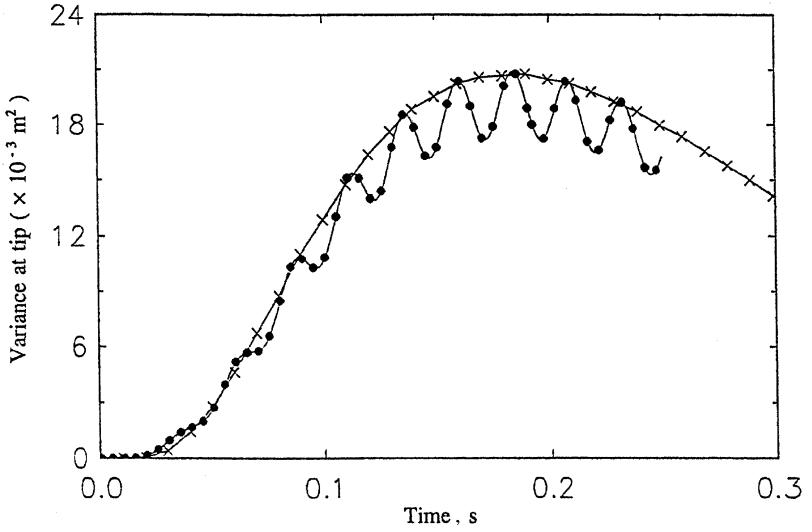

Fig. 10. Resonant displacement response of discretized beam under narrow band random excitation with $\omega_f = 130.0$ rad/s, $\zeta_f = 0.05$; MCS (•), and SCD (×).

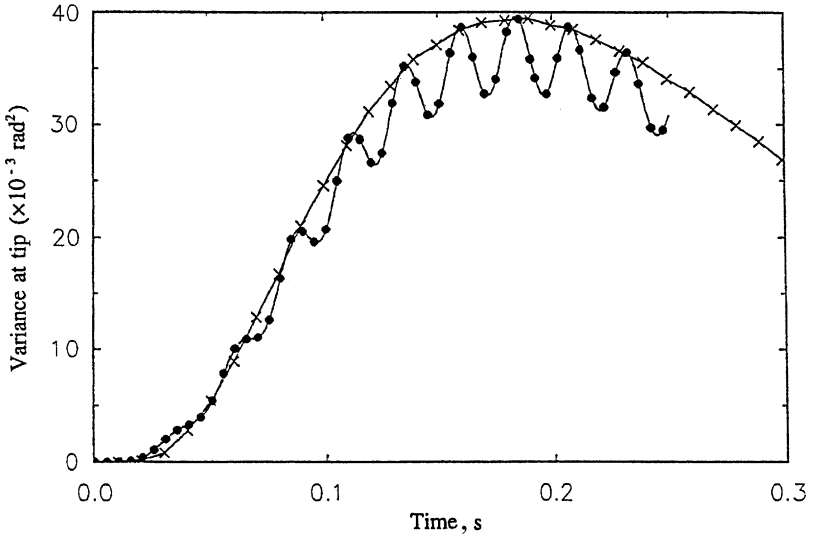

Fig. 11. Resonant rotation response of discretized beam under narrow band random excitation with $\omega_f = 130.0\,\text{rad/s}$, $\zeta_f = 0.05$. MCS (•), and SCD (×).

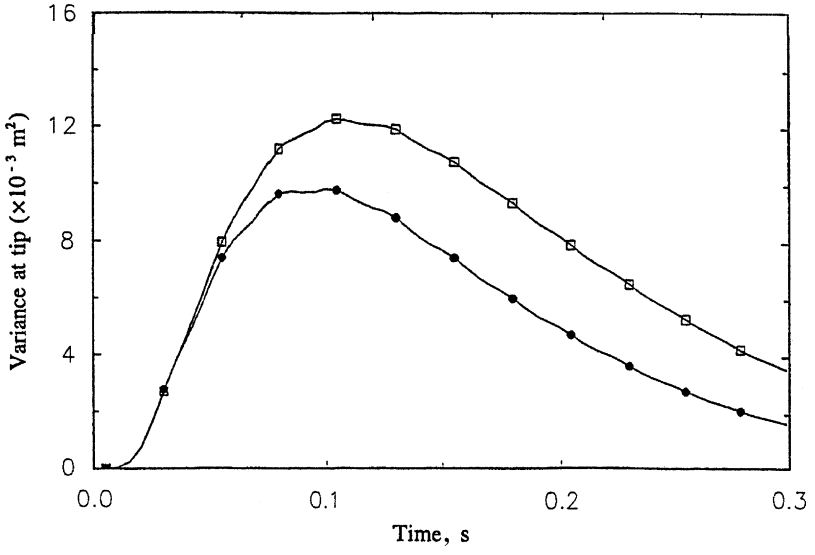

Fig. 12. Effect of bandwidth on displacement responses of discretized cantilever beam with $\omega_f = 130.0\,\text{rad/s}$, $\zeta_f = 0.05$ (□), and $\zeta_f = 0.1$ (•).

characteristics mentioned in the last subsection are applied here. The modulating function $e(t)$ of the narrow band nonstationary random excitation given by Eq. (21a) is the same as that defined in Eq. (23). However, $(I_f)^{1/2}$ in Eq. (21a) is such that $I_f = 2\pi \times 10^4$.

Computed results are presented in Figs. 12 and 13. With reference to the figures, one observes that the system response increases with decreasing band width of the random excitation process.

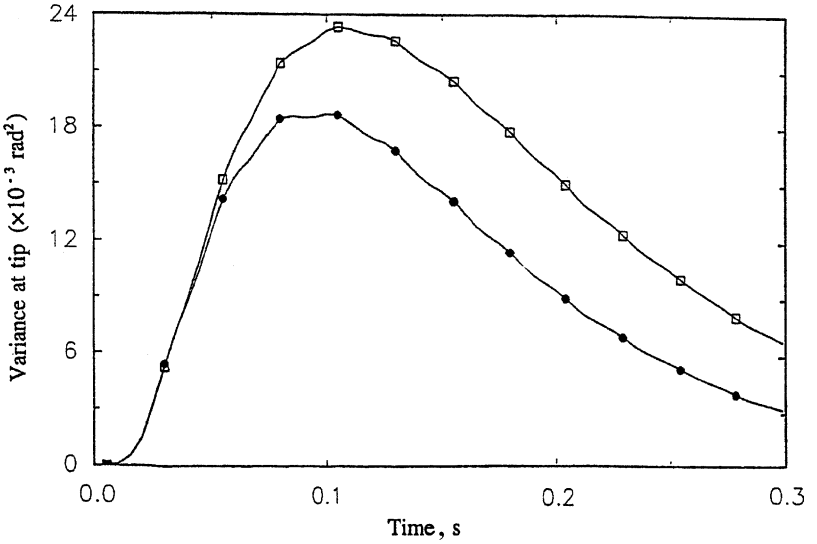

Fig. 13. Effect of bandwidth on rotation responses of discretized cantilever beam with $\omega_f = 130.0\,\mathrm{rad/s}$, $\zeta_f = 0.05$ (□), and $\zeta_f = 0.1$ (•).

5. Flow-induced vibration of a uniform pipe

Aside from further demonstration of application of the ESCD for a structure discretized by the FEM, the flow-induced vibration of a uniform pipe containing a moving medium [15–17] is a good example of a discretized system with nonproportional damping. The damping matrix in such a system is skew symmetric. The computed results by using the ESCD method are compared with those applying the MCS.

5.1. Water flowing in a straight pipe

The particular example considered is a straight uniform pipe containing flowing water. It is pin-supported at both ends [18]. For illustration purpose, the structure shown in Fig. 14 is approximated by two 2-node beam bending elements. It may be appropriate to mention that the coarse finite element mesh used here is mainly for illustration rather than attempting to present an accurate practical solution to the problem. Each node of the element has 2 dof namely transversal deflection and rotation. The motion in the system shown in Fig. 14 is such that the consistent element mass, damping and stiffness matrices of a pipe containing running fluid are

$$[m] = \frac{(m_p + m_f)\ell}{420}\begin{bmatrix} 156 & 22\ell & 54 & -13\ell \\ 22\ell & 4\ell^2 & 13\ell & -3\ell^2 \\ 54 & 13\ell & 156 & -22\ell \\ -13\ell & -3\ell^2 & -22\ell & 4\ell^2 \end{bmatrix}, \tag{25}$$

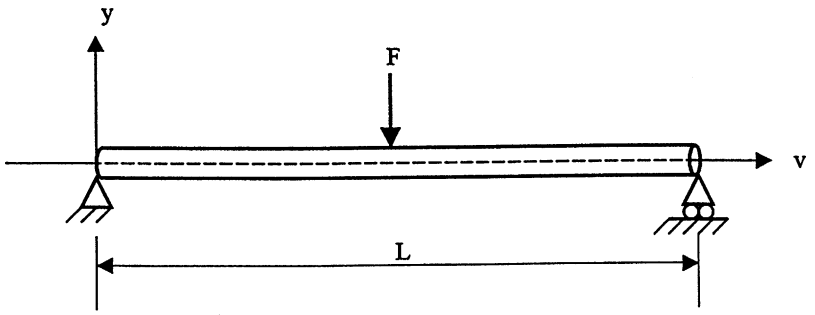

Fig. 14. A fluid-conveying pipe with pinned ends.

$$[c] = \frac{m_f v}{30}\begin{bmatrix} 0 & 6\ell & 30 & -6\ell \\ -6\ell & 0 & 6\ell & -\ell^2 \\ -30 & -6\ell & 0 & 6\ell \\ 6\ell & \ell^2 & -6\ell & 0 \end{bmatrix}, \tag{26}$$

$$[k_o] = \frac{EI_b}{\ell^3}\begin{bmatrix} 12 & 6\ell & -12 & 6\ell \\ 6\ell & 4\ell^2 & -6\ell & 2\ell^2 \\ -12 & -6\ell & 12 & -6\ell \\ 6\ell & 2\ell^2 & -6\ell & 4\ell^2 \end{bmatrix}, \tag{27}$$

$$[k_f] = \frac{m_f v^2}{30\ell}\begin{bmatrix} 36 & 3\ell & -36 & 3\ell \\ 3\ell & 4\ell^2 & -3\ell & -\ell^2 \\ -36 & -3\ell & 36 & -3\ell \\ 3\ell & -\ell^2 & -3\ell & 4\ell^2 \end{bmatrix}, \tag{28}$$

where m_p is the mass per unit length of the pipe, m_f is the mass per unit length of the fluid, E is Young's modulus of the pipe material, I_b is the moment of inertia of the pipe cross-section area, ℓ is the length of finite element, and v is the velocity of the fluid inside the pipe.

Based on consistent element matrices $[m]$, $[c]$ and $[k] = [k_o] - [k_f]$, the assembled mass, damping, and stiffness matrices can be obtained as

$$[M] = \sum_{e=1}^{N+1} [M]_e, \quad [C] = \sum_{e=1}^{N+1} [C]_e, \quad [K] = \sum_{e=1}^{N+1} [K]_e, \tag{29}$$

where the subscript e denotes the element number; $[M]_e$, $[C]_e$ and $[K]_e$ have the same order as the assembled mass matrix $[M]$, damping matrix $[C]$, and stiffness matrix $[K]$, respectively. The nonzero elements in the latter matrices are only those in rows and columns that correspond to element degrees of freedom. After assembling and applying the boundary conditions, the resultant size of the mass, damping and stiffness matrices is four by four.

The structure is subjected to a concentrated narrow band nonstationary random excitation at its mid-span. The governing matrix equation of motion in terms of the global displacement,

velocity and acceleration vectors is similar to Eq. (20). The excitation for this particular problem is defined by Eq. (21).

5.2. Narrow band nonstationary random responses

A number of numerical tests was conducted to examine the efficiency and accuracy of the ESCD method for the response statistics of the flow-induced vibration problem. The material properties of the pipe are: Young's modulus $E = 68.5\,\text{GPa}$, pipe outer radius $r_p = 26.0\,\text{mm}$, pipe thickness $h = 3.5\,\text{mm}$, pipe total length $L = 2.8\,\text{m}$, $m_f = 1.59\,\text{kg/m}$, $m_p = 1.49\,\text{kg/m}$, $v = 38\,\text{m/s}$. The corresponding undamped frequencies are $\omega_1 = 68.5\,\text{rad/s}$, $\omega_2 = 325.9\,\text{rad/s}$, $\omega_3 = 828.3\,\text{rad/s}$ and $\omega_4 = 1514.7\,\text{rad/s}$. The center frequency of the filter is selected in such a way that it mainly excites the fundamental mode of the pipe. The center frequency ω_f and damping ratio ζ_f of the filter are 89.0 rad/s and 0.05, respectively. The sdof filter is excited by a modulated Gaussian white noise process. The latter is given by

$$P(t) = e(t)w(t), \quad \langle w^2(0)\rangle = 2\pi \times 10^9, \quad e(t) = 9.4815(\mathrm{e}^{-45t} - \mathrm{e}^{-60t}). \tag{30}$$

The results of variances of responses by the ESCD method, in which $\Delta\tau = 1.0$, are presented in Figs. 15–17 in which they are denoted as SCD. Results obtained by the MCS are also included in these figures for comparison. In the MCS the number of realizations applied was 150. It may be worth pointing out that a number of resonant cases were tested and the responses were unbounded. These are associated with the so-called flutter instability which is not the objective of the current investigation and therefore are not pursued further here. Note that the magnitudes of nonresonant variances of displacement and rotation or angular displacement responses in Figs. 15–17 are reasonable in that they are within the linear ranges.

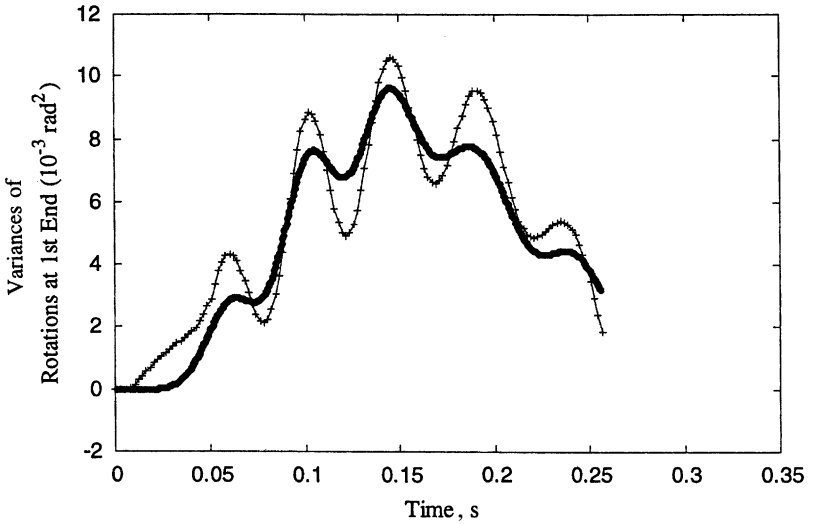

Fig. 15. Variances of rotation responses at left end with $\omega_f = 89.0\,\text{rad/s}$, $\zeta_f = 0.05$. Simulation (•), and SCD (+).

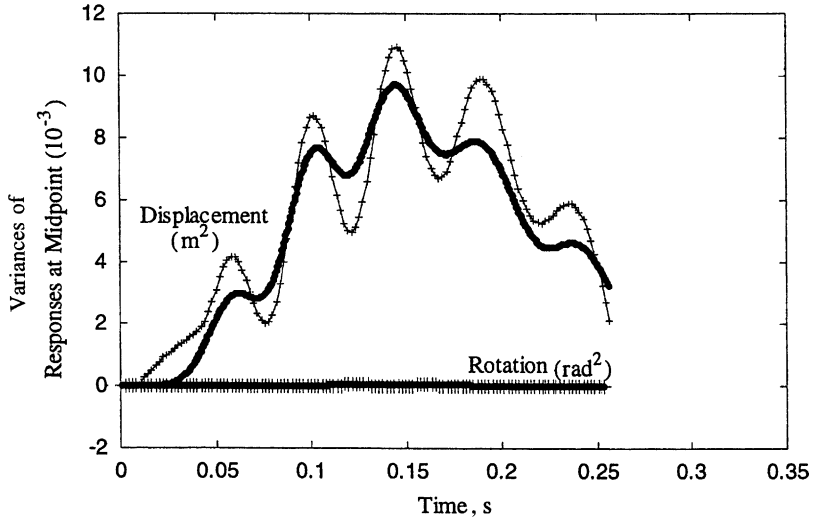

Fig. 16. Variances of responses at midpoint of pipe with $\omega_f = 89.0\,\text{rad/s}$, $\zeta_f = 0.05$. Simulation (•), and SCD (+).

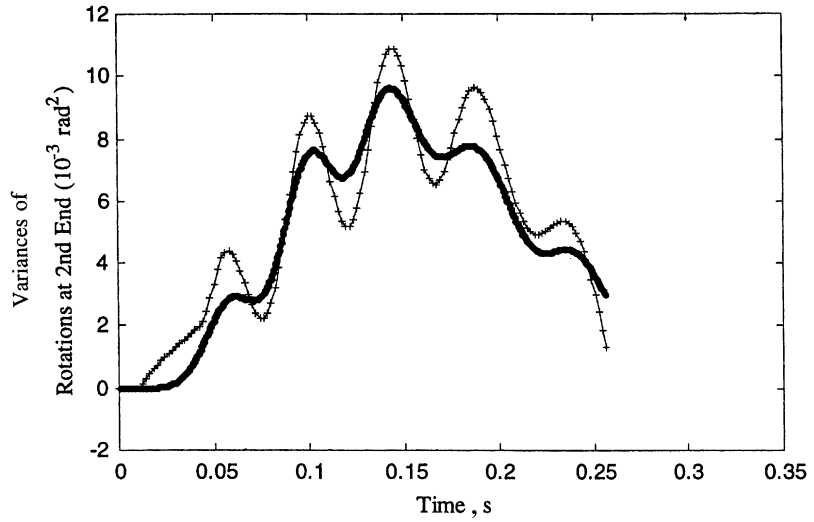

Fig. 17. Variances of rotations at right end of pipe with $\omega_f = 89.0\,\text{rad/s}$, $\zeta_f = 0.05$. Simulation (•), and SCD (+).

It may be of interest to note that for every case the computation time required by the ESCD method is about 1.0 s while that by the MCS is approximately 8 min on a dual pentium II 266 MHz machine.

With reference to the figures presented in this subsection, one could conclude that the ESCD method is applicable to nonproportional damping problems and that the ESCD method is very efficient and accurate even for a system with only 4 dof. This implies that for practical systems that have a large number of dof, computation time saved by the ESCD method can be very significant.

5.3. Effect of bandwidth of excitation processes

The purpose of the study included in this subsection is to examine the effect of bandwidth of the excitation process from the single dof filter on the responses of the pipe. The filter characteristics mentioned in the last subsection is employed here. The modulating function $e(t)$ of the narrow band nonstationary random excitation given in Eq. (21a) is the same as that defined in Eq. (23), while $(I_f)^{1/2}$ in Eq. (21a) is such that $I_f = 2\pi \times 10^4$.

Computed results are presented in the figures. Two pipes with different properties were adopted. The first one is made of aluminum which was used in the previous subsection. The center frequency of filter applied is 37.6 rad/s and the results are presented in Figs. 18–20. The second example is a steel pipe whose properties are as follow: Young's modulus $E = 200\,\text{GPa}$, pipe outer radius $r_p = 26.0\,\text{mm}$, pipe thickness $h = 3.5\,\text{mm}$, pipe total length $L = 2.8\,\text{m}$, $m_f = 1.59\,\text{kg/m}$, $m_p = 4.19\,\text{kg/m}$, $v = 38\,\text{m/s}$. The corresponding undamped frequencies are $\omega_1 = 90.6\,\text{rad/s}$, $\omega_2 = 410.2\,\text{rad/s}$, $\omega_3 = 1035\,\text{rad/s}$ and $\omega_4 = 1888.9\,\text{rad/s}$. A narrow band random excitation with center frequency of 80.0 rad/s was applied to the pipe at the midpoint. Figs. 21–23 contain the responses of the pipe.

With reference to the figures, one observes that the system responses increase with decreasing bandwidth of the random excitation process, which are consistent with the results presented in previous sections. Before closing this subsection, it should be noted that even for the coarse mesh finite element model of flow-induced vibration of pipe containing a moving medium and subjected to a narrow band nonstationary random excitation no similar work can be found in the literature.

6. Concluding remarks

The new feature in the presently proposed ESCD method is its efficient capability of dealing with narrow band stationary and nonstationary random excitations applied to the structures

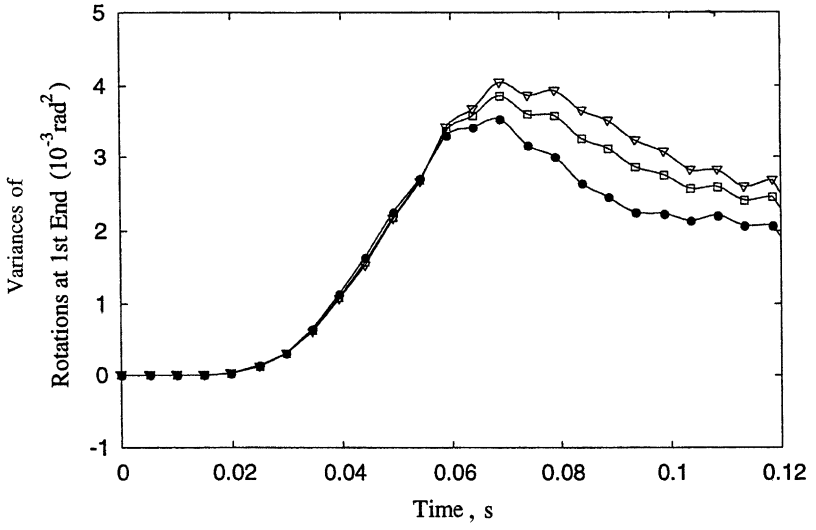

Fig. 18. Effect of bandwidth on variances of rotations at left end with $\omega_1 = 68.5\,\text{rad/s}$, $\omega_f = 89.0\,\text{rad/s}$; $\zeta_f = 0.025$ (▽), $\zeta_f = 0.05$ (□), and $\zeta_f = 0.1$ (•).

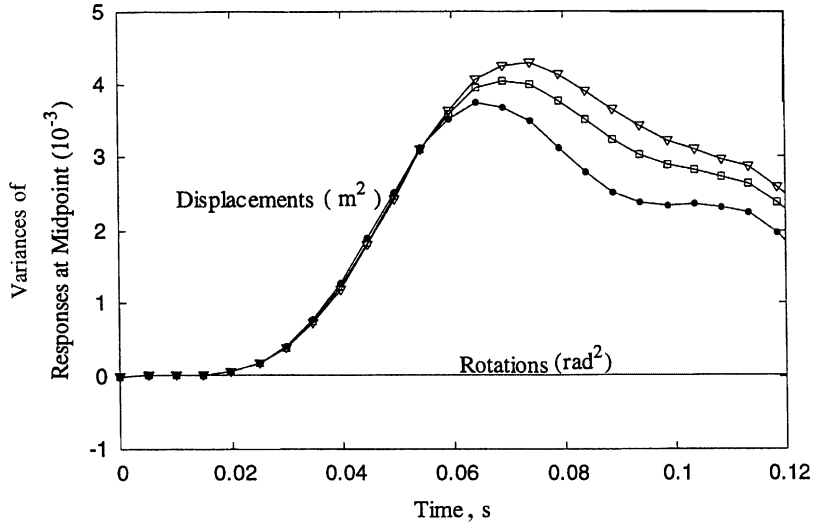

Fig. 19. Effect of bandwidth on variances of responses at midpoint of beam with $\omega_1 = 68.5\,\text{rad/s}$, $\omega_f = 89.0\,\text{rad/s}$; $\zeta_f = 0.025$ ($\triangledown$), $\zeta_f = 0.05$ ($\square$), and $\zeta_f = 0.1$ ($\bullet$).

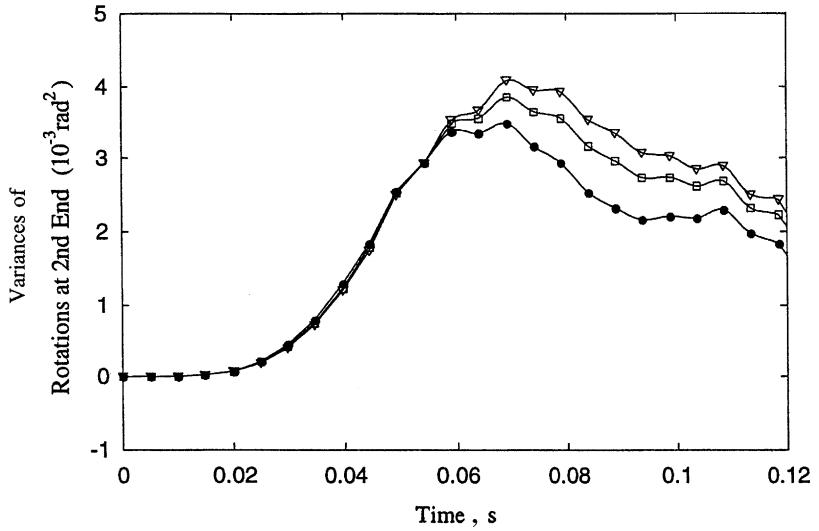

Fig. 20. Effect of bandwidth on variances of rotation responses at right end with $\omega_1 = 68.5\,\text{rad/s}$, $\omega_f = 89.0\,\text{rad/s}$; $\zeta_f = 0.025$ ($\triangledown$), $\zeta_f = 0.05$ ($\square$), and $\zeta_f = 0.1$ ($\bullet$).

approximated by the FEM. It also provides a means of controlling the center frequencies and band widths of narrow band stationary and nonstationary random excitations.

By applying different envelope functions $e_f(s)$, constant I, the natural frequencies of the filter and the ratios of damping to mass, a variety of different shapes, spectral densities, center

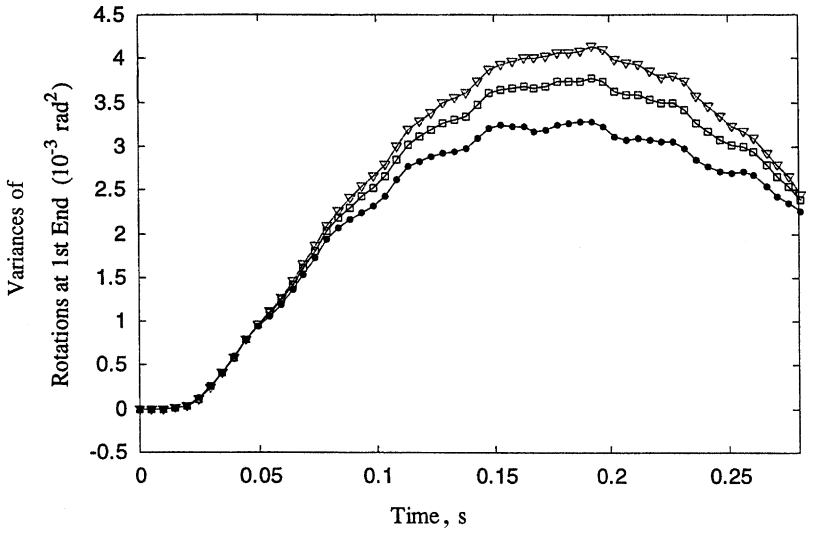

Fig. 21. Effect of bandwidth on variances of rotation responses at left end with $\omega_1 = 90.6\,\text{rad/s}$, $\omega_f = 80.0\,\text{rad/s}$; $\zeta_f = 0.01$ (∇), $\zeta_f = 0.025$ ($\square$), and $\zeta_f = 0.05$ ($\bullet$).

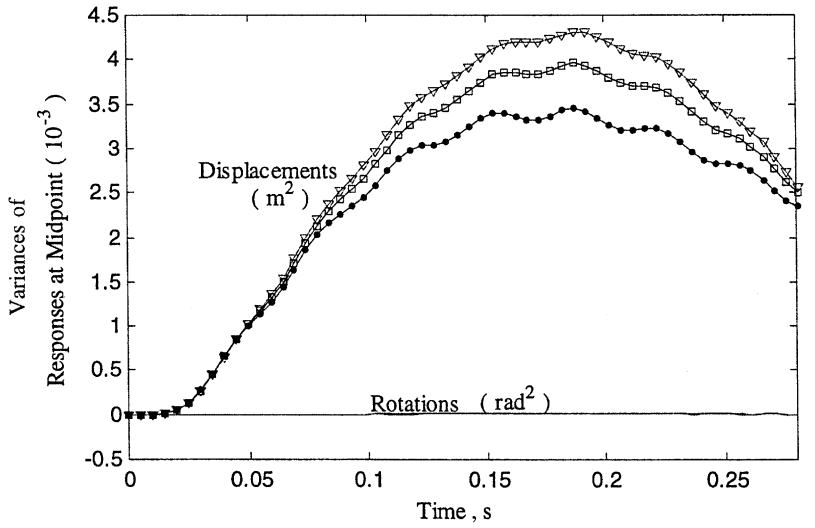

Fig. 22. Effect of bandwidth on variances of responses at midpoint with $\omega_1 = 90.6\,\text{rad/s}$, $\omega_f = 80.0\,\text{rad/s}$; $\zeta_f = 0.01$ (∇), $\zeta_f = 0.025$ ($\square$), and $\zeta_f = 0.05$ ($\bullet$).

frequencies and band widths of the narrow band random processes from the filter can be obtained. This is a unique feature which the well established MCS cannot provide.

The proposed ESCD method is suitable for large-scale random response analysis of complicated structures as it applies the FEM. Furthermore, it does not require the normal mode

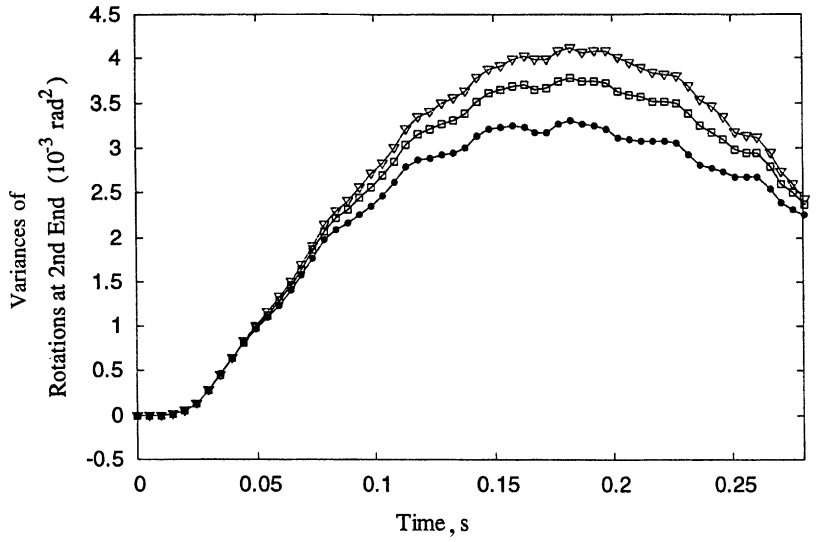

Fig. 23. Effect of bandwidth on variances of rotation responses at right end with $\omega_1 = 90.6\,\text{rad/s}$, $\omega_f = 80.0\,\text{rad/s}$; $\zeta_f = 0.01$ ($\triangledown$), $\zeta_f = 0.025$ ($\square$), and $\zeta_f = 0.05$ ($\bullet$).

or complex normal mode analysis or direct numerical integration algorithms such as the fourth-order Runge–Kutta scheme.

Computed results of several examples were obtained. It is believed that for the first time responses of a uniform pipe containing a moving medium and excited by a narrow band nonstationary random disturbance has been evaluated by applying the FEM. Computed results show that: (1) differences between the responses of discretized systems under narrow band and wide band random excitations can be very significant and therefore a correct representation of the excitation processes is of paramount important, (2) the proposed method is very accurate and efficient compared with those obtained by using the MCS, and (3) because of its recursive nature and the fact that it is based on the FEM it can be generalized to deal with the nonlinear random response of discretized systems. Such a generalization and its application to nonlinear random response analysis will be presented in a companion paper [9].

References

[1] C.W.S. To, The stochastic central difference method in structural dynamics, *Computers and Structures* 23 (1986) 813–818.
[2] J.B. Roberts, P.D. Spanos, *Random Vibration and Statistical Linearization*, Wiley, New York, 1990.
[3] C.W.S. To, A stochastic version of the Newmark family of algorithms for discretized dynamic systems, *Computers and Structures* 44 (3) (1992) 667–673.
[4] C.W.S. To, The response of non-linear structures to random excitation, *Shock and Vibration Digest* 16 (4) (1984) 13–32.
[5] S. Rajan, Random Superharmonic and Subharmonic Response of a Duffing Oscillator, Ph.D. Thesis, The University of New Brunswick, February 1987.

[6] W.C. Lennox, Y.C. Kuak, Narrow band excitation of a non-linear oscillator, *Journal of Applied Mechanics* 43 (1976) 340–344.
[7] G. Tagata, Analysis of a randomly excited non-linear stretched string, *Journal of Sound and Vibration* 58 (1) (1978) 95–107.
[8] C.W.S. To, Techniques for response analysis of nonlinear systems under random excitations, *Shock and Vibration Digest* 23 (11) (1991) 3–15.
[9] Z. Chen, C.W.S. To, Responses of discretized systems under narrow band nonstationary random excitations. Part 2: nonlinear problems, *Journal of Sound and Vibration* 287 (3) (2005) 459–479, this issue; doi:10.1016/j.jsv.2004.11.021.
[10] M.L. Liu, Response Statistics of Shell Structures with Geometrical and Material Nonlinearities, Ph.D. Thesis, University of Western Ontario, 1993.
[11] M.L. Liu, C.W.S. To, Adaptive time schemes for responses of non-linear multi-degree-of-freedom systems under random excitations, *Computers and Structures* 52 (3) (1994) 563–571.
[12] C.W.S. To, M.L. Liu, Random responses of discretized beams and plates by the stochastic central difference method with time co-ordinate transformation, *Computers and Structures* 53 (3) (1994) 727–738.
[13] T.T. Soong, *Random Differential Equations in Science and Engineering*, Academic Press, New York, 1973.
[14] G.B. Warburton, *The Dynamical Behaviour of Structures*, second ed., Pergamon Press, Oxford, 1976.
[15] C.W.S. To, J.W. Healy, Further comment on vibration analysis of straight and curved tubes conveying fluid by means of straight beam finite elements, *Journal of Sound and Vibration* 105 (3) (1986) 513–514.
[16] A. Pramila, Comment on vibration analysis of straight and curved tubes conveying fluid by means of straight beam finite elements, *Journal of Sound and Vibration* 99 (2) (1985) 293–294.
[17] A.K. Kohli, B.C. Nakra, Vibration analysis of straight and curved tubes conveying fluid by means of straight beam finite elements, *Journal of Sound and Vibration* 93 (2) (1984) 307–311.
[18] R.D. Blevins, *Flow Induced Vibration*, second ed., Van Nostrand Reinhold, New York, 1990.